Development of a Performance Assessment Model: Lecture Notes

K. Huff
khuff@cae.wisc.edu

Contents

1   Groundwater Hydrology [1, 2]

Groundwater hydrology is the study of groundwater movement.

1.1   Hydraulic Head

Hydraulic head is the hydrologic indicator of potential energy. It has units of length, specifically height above a geological *datum*, the zero point relative to which heads are measured.

One way to derive this notion is according to Hubbart's derivation [2]. The work to raise the water to a pressure, P, and the work required to raise the water to an elevation, z, are additive.

The work required to raise a mass, m, to a pressure, P, is described by the integral

$$W_P = \frac{1}{m} \int_0^P V dP \tag{1}$$

where

$$
\begin{aligned}
m &= \text{ mass of the water } [kg] \\
V &= \text{ volume of the water } [m^3] \\
P &= \text{ pressure } [kg/m/s^2].
\end{aligned}
$$

In an incompressible fluid such as water, the work W_P required to raise a unit mass to some pressure, P, becomes

$$W_P = P/\rho_w \tag{2}$$

where

$$\rho_w = \text{ the density of water} [kg/m^3].$$

The work required to raise a unit mass to elevation z from elevation z_{ref} (the 'datum') is simply the work, W_g against gravity

$$W_g = g(z - z_{ref}) \tag{3}$$

where

$$g = \text{ acceleration of gravity } [m/s^2].$$

From these expressions for work the potential energy function, ϕ, of the two separate potentials, pressure and elevation, act additively on a unit mass of groundwater. Their combined effects can be written as the sum,

$$
\begin{aligned}
\phi &= W_P + W_g \\
&= \frac{P}{\rho_w} + g(z - z_{ref}.)
\end{aligned}
\tag{4}
$$

If

$$z_{ref} = 0$$

and the potential energy is directly proportional to gravity

$$\phi = gh$$

where

$$h = \text{Darcy's experimental head } [m],$$

then

$$
\begin{aligned}
h &= \frac{\phi}{g} \\
&= \frac{P}{\rho_w g} + z \\
&= \psi + z
\end{aligned}
\tag{5}
$$

where

$$z = \text{elevation head } [m]$$
$$\psi = \text{pressure head } [m].$$

Thus, the total hydraulic head, h, of a column of water is the vertical distance from the datum ($h = 0$) to the height of the water surface. Elevation head, z, is the distance from the datum to the measuring point in the flow field. The pressure head, ψ, is the pressure, P in $[Pa]$, at that measurement point, divided by the density of the fluid, ρ_w, and the accelation of gravity, g. Pressure head, elevation head, and total head are shown in Figure 1.
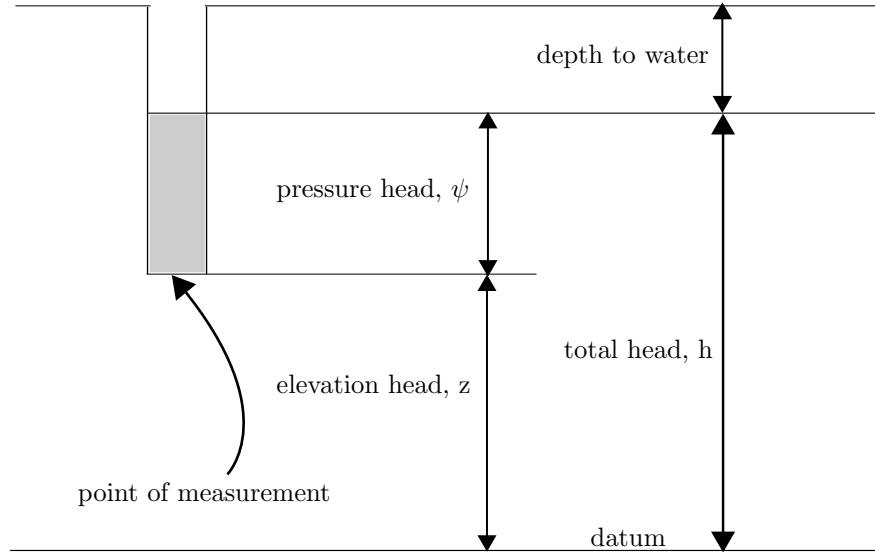
Figure 1: Various types of head value in a column of water in a well are measured with respect to the datum.

Different lithologies and candidate sites have different head gradients. Due to anisotropies in their hydraulic conductivity tensors (see section 1.4), some lithologies, such as clay, are less likely to have strong head gradients.

1.2   Porosity

Porosity is a hydraulic parameter which significantly contributes to the hydraulic conductivity of a medium.

The porosity of a medium is the ration of void volume, V_v, in the medium to the total volume, V_T of the medium. As shown in Figure 2, the volume of water sufficient to saturate a packed sand matrix is equivalent to the void volume.
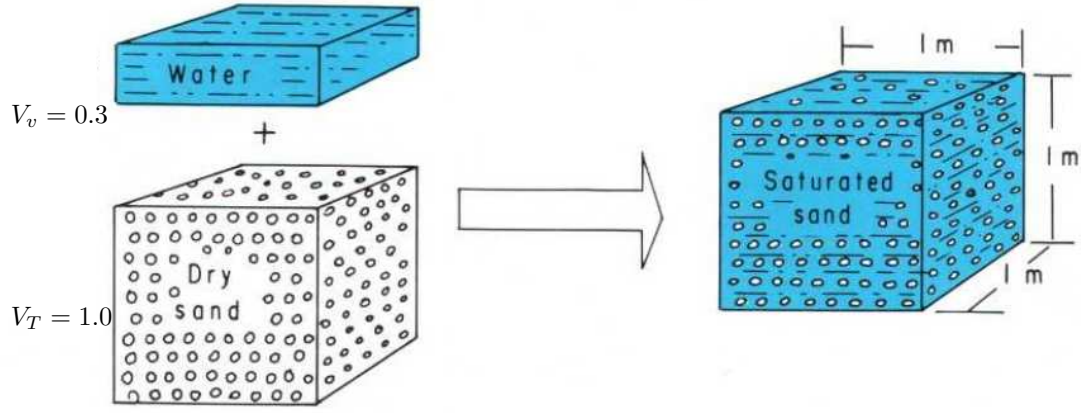
$$\text{Porosity(n)} = \frac{\text{Volume of Voids}_{(V_v)}}{\text{Total Volume}_{(V_T)}} = \frac{0.3m^3}{1.0m^3} = 0.3$$

Figure 2: The ratio of the volume of saturation water to the total packed sand volume gives the porosity, n, in [%] [5].

The porosity of a material is therefore mathematically defined as

$$
\begin{aligned}
n_T &= \frac{\text{void volume}}{\text{total volume}} \\
&= \frac{V_v}{V_T} \\
&= \frac{V_T - V_s}{V_T}
\end{aligned}
\tag{6}
$$

where

$$
\begin{aligned}
n_T &= \text{ total porosity } [\%] \\
V_v &= \text{ void volume } [m^3] \\
V_T &= \text{ total volume } [m^3] \\
V_s &= \text{ volume of solids } [m^3].
\end{aligned}
$$

The dry solid volume can be defined as

$$V_s = \frac{m_s}{\rho_s} \tag{7}$$

and the total dry volume can be defined as

$$V_T = \frac{m_s}{\rho_b}, \tag{8}$$

where

$$
\begin{aligned}
\rho_s &= \text{ grain density, or density of solids } [kg/m^3] \\
m_s &= \text{ mass of solids } [kg]
\end{aligned}
$$

and

$$\rho_b = \text{ bulk (dry) density } [kg/m^3],$$

equation (6) can be rewritten

$$n_T = 1 - \frac{\rho_b}{\rho_s}. \tag{9}$$

The total porosity is a combination of primary and secondary porosity, shown in Figure 3. Primary porosity is the macroscopically homogeneous void space present between grains in a geological matrix. This type of porosity includes empty space between grains of sand or consolidated rock characteristic of the level of packing or method of consolidation of the matrix. Secondary porosity is not intrinsic to the rock, but induced in it. Examples of secondary porosity include features such as fractures, lava tubes, and caverns.
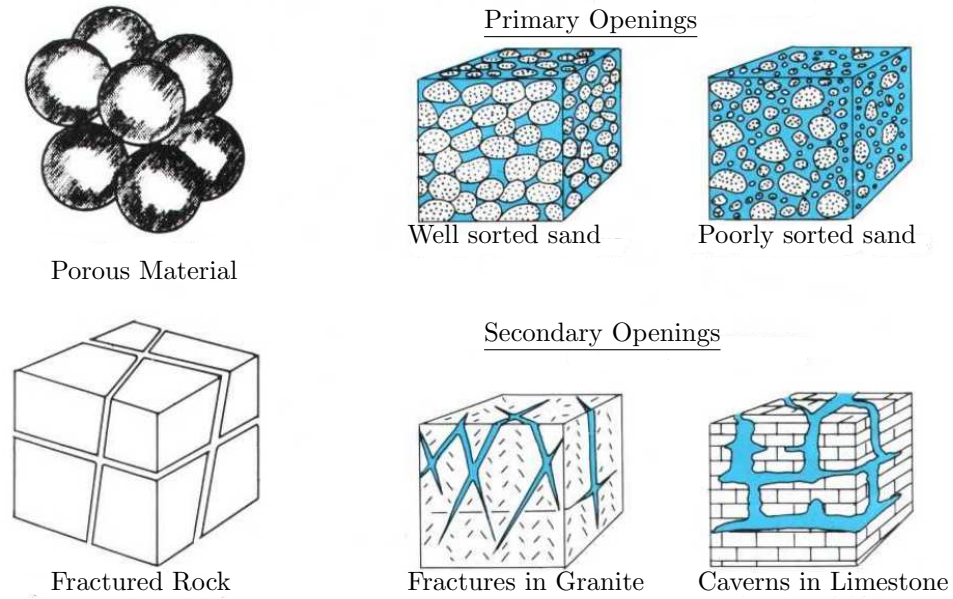
Figure 3: Primary porosity, a homogeneous characteristic of the rock matrix, and secondary porosity, such as discrete fractures, caverns, and lava tubes, both contribute to total porosity [5].

Equipped with a notion of the total porosity, it is possible to define the effective porosity shown in figure 4, which is the interconnected porosity through which fluid may flow,

$$n_{eff} = \frac{V_c}{V_T} n_T. \tag{10}$$

where

$$V_c = \text{ interconnected volume.}$$

Effective porosity is more influential on ground water flow in a porous medium than the total porosity, as it contributes to the permeability of the medium. In some media, the effective porosity is significantly different than the total porosity, resulting in much lower flow rates than the total porosity alone would indicate. Granite, for example, has an effective porosity that is nearly three magnitudes lower than its total porosity.

"poorly" connected pore volume

$n_{eff} \ll n_T$

$n_{eff} \sim n_T$

"well" connected pore volume
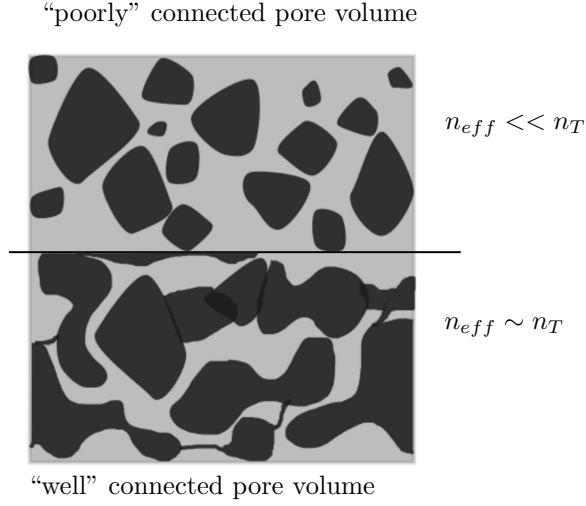
Figure 4: A medium with a poorly connected pore volume has low effective porosity, and vice versa.

1.3 Darcy's Law

Darcy's Law is analgous to Fourier's Law of heat conduction, and states that flow occurs as a function of a head gradient with a speed that obeys the hydraulic properties of the medium. Darcy's law for one dimensional flow is

$$\frac{Q}{A} = -K\frac{h_2 - h_1}{l_2 - l_1} \tag{11}$$

where

$$Q = \text{ volumetric flow rate } [m^3/s]$$

and

$$
\begin{aligned}
A &= \text{ cross sectional area of flow field } [m^2] \\
K &= \text{ hydraulic conductivity } [m/s]. \\
h_i &= \text{ hydraulic head measured at point i } [m] \\
l_i &= \text{ linear position of point i } [m]
\end{aligned}
$$

Using the the definition of specific discharge (also known as Darcy flux), $q = Q/A$, and expressing the law in its differential form gives

$$q = -K\frac{\partial h}{\partial l}. \tag{12}$$

The three dimensional form requires that the one dimensional form in equation (12) be true for each spatial component, such that

$$\vec{q} = -K\nabla h \tag{13}$$

where

$$
\begin{aligned}
\vec{q} &= \text{ specific discharge vector } [m^3/s] \\
&= q_x\hat{i} + q_y\hat{j} + q_z\hat{k}
\end{aligned}
$$

6

and

$$\nabla h = \frac{\partial h}{\partial x} + \frac{\partial h}{\partial y} + \frac{\partial h}{\partial z}.$$

In the case of anisotropic media, the hydraulic conductivity, K is given as a spatially heterogenous tensor, $\mathbf{K}$. The general, three dimensional, anisotropic Darcy equation is therefore

$$\vec{q} = -\mathbf{K}\nabla h \tag{14}$$

where

$$\mathbf{K} = \text{ hydraulic conductivity tensor } [m/s].$$

1.4 Hydraulic Conductivity

The hydraulic conductivity of a medium is a tensor that describes the ease with which water passes through the pore spaces of the medium in all directions. This tensor may be homogeneous or heterogeneous and isotropic or anisotropic.

1.4.1 Heterogeneity of the Hydraulic Conductivity

Heterogeneity of a hydrogeological unit describes the spatial variability of the hydraulic conductivity. If the hydraulic conductivity is the same when measured at all points in the hydrogeological medium,

$$\forall i, j \in V : K(x_i, y_i, z_i) = K(x_j, y_j, z_j), \tag{15}$$

then the medium is homogenous. If instead, the hydraulic conductivity is different at different locations, such that

$$\exists i \neq j \in V : K(x_i, y_i, z_i) \neq K(x_j, y_j, z_j), \tag{16}$$

then the medium is heterogeneous.

1.4.2 Anisotropy of the Hydraulic Conductivity

Anisotropy of a hydrogeological unit describes the local directional dependence of the hydraulic conductivity tensor. Specifically, at a single location, an isotropic medium will demonstrate the same hydraulic conductivity in all directions, while an anisotropic medium will not.

Mathematically speaking, if the conductivity is constant at all measurement angles, θ, such that

$$\forall \theta_i, \theta_j \in (0, 2\pi) : K(\theta_i, x, y, z) = K(\theta_j, x, y, z) \tag{17}$$

$$\tag{18}$$

then the medium is isotropic. If instead, the angular components of the hydraulic conductivity are nonconstant, such that

$$\exists \theta_i \neq \theta_j \in (0, 2\pi) : K(\theta_i, x, y, z) \neq K(\theta_j, x, y, z), \tag{19}$$

then the medium is anisotropic and the tensor is expressed most generally,

$$\mathbf{K} = \text{ hydraulic conductivity tensor } [m/s]$$
$$= \begin{bmatrix} K_{xx} & K_{xy} & K_{xz} \\ K_{yx} & K_{yy} & K_{yz} \\ K_{zx} & K_{zy} & K_{zz} \end{bmatrix} \tag{20}$$

where

$$K_{ij} = \text{jth component in the i direction.}$$

The general tensor in equation (20) is a second rank symmetric tensor and can always be simplified by aligning the tensor with the principal axis of anisotropy[1]. This principal direction is defined by the directions of maximum $(K_\parallel)$, minimum $(K_\perp)$, and intermediate $(K_\parallel \times K_\perp)$ hydraulic conductivity. That is, by aligning the tensor with the flow axis, it may be reduced to a diagonal matrix,

$$\mathbf{K} = \left[\begin{array}{ccc} K_{xx} & 0 & 0 \\ 0 & K_{yy} & 0 \\ 0 & 0 & K_{zz} \end{array} \right]. \tag{21}$$

2 Mechanisms of Solute Transport

Solutes in groundwater are transported due to various mechanisms.

2.1 Diffusion

Solutes will move from a location of high concentration to a location of low concentration due to the random thermal kinetic enery of the solute. Brownian motion is responsible for diffusion.
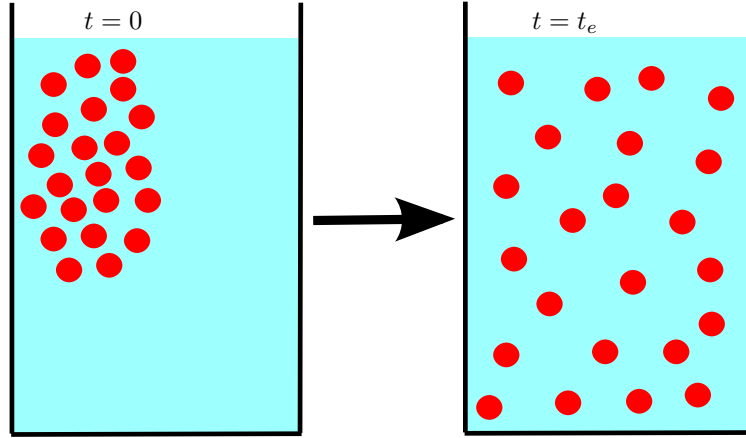
Figure 5: In diffusive transport, particles move according to random thermal motion down the concentration gradient [6].

A mathematical description of this phenomenon can be addressed by describing the particle's motion as a random walk and applying statistical analysis. Another derivation of this phenomenon describes the flux, J through a plane in a volume, and gives Fick's Law for porous media,

$$J_{xdif} = -D'\frac{dC}{dx}$$

$$\tag{22}$$

where

$$
\begin{aligned}
J_x &= \text{ Mass flux through the y-z plane } [kg/m^2/s] \\
D' &= \text{ Effective diffusion coefficient } [m^2/s] \\
C &= \text{ Concentration } [kg/m^3].
\end{aligned}
$$

(23)

The determination of the diffusion coefficient can be empirical or analytical. The Arrhenius equation gives a thermal dependence of the diffusion coefficient as does the Stokes-Einstein relationship.

The effecive diffusion coefficient for porous media is dependent on porosity and tortuosity, which affect the diffusion behavior of a solute. In a saturated porous medium, diffusion takes place only within the pore volume where liquid is present. To take this into account, the effective diffusion coefficient in a porous medium is reduced by both the absence of fluid in the matrix volume, and by the so-called "tortuosity" of the pathways.

$$
J_{xdif} = -n\tau D_m \frac{dC}{dx} \tag{24}
$$

(25)

where

$$
\begin{aligned}
J_{xdif} &= \text{ Mass flux through the y-z plane in a porous medium} [kg/m^2/s] \\
n &= \text{ porosity } [\%] \\
\tau &= \text{ tortuosity } [-] \\
D_m &= \text{ Molecular diffusion coefficient } [m^2/s] \\
C &= \text{ Concentration } [kg/m^3].
\end{aligned}
$$

The tortuosity of a saturated porous medium can be estimated from the porosity with an equation developed by Millington and Quirk (1961),

$$
\tau = \frac{n_w^{7/3}}{n^2} \tag{26}
$$

which for a saturated medium is estimated as

$$
\tau = n^{1/3}. \tag{27}
$$

(28)

2.2 Dispersion [1]

Solutes can be driven to move due to mechanical mixing, known as dispersion. Solutes acting under dispersion may travel further than they would due to advection alone. During fluid mixing in which a fluid with one solute concentration displaces a fluid with another concentration, dispersion causes a zone of mixing to develop around the advective front.

Dispersion in groundwater is caused by a combination of two phenomena. The first is mechanical dispersion, in which local variability of the fluid velocity around the mean due to mechanical heterogeneities of the rock at many scales. The second phenomenon is diffusion, discussed in section 2.1.

A mathematical description of this phenomenon will come generally from fluid dynamics. The total mechanical dispersive and diffusive phenomena can be combined as a total dispersive expression,

$$
D = D_{mdis} + \tau D_m \tag{29}
$$

9

where

$$
\begin{aligned}
D_{mdis} =\ & \text{coefficient of mechanical dispersivity } [m^2/s] \\
=\ & \alpha_L \frac{v_x^2}{|v|} + \alpha_{TH} \frac{v_y^2}{|v|} + \alpha_{TV} \frac{v_z^2}{|v|},
\end{aligned}
\tag{30}
$$

$$
\begin{aligned}
\alpha_L =\ & \text{longitudinal dispersivity } [m], \\
\alpha_{TH} =\ & \text{horizontal transverse dispersivity } [m], \\
\alpha_{TV} =\ & \text{vertical transverse dispersivity } [m], \\
\tau =\ & \text{tortuosity } [-],
\end{aligned}
$$

and

$$
D_m = \text{coefficient of molecular diffusion } [m^2/s].
$$

The dispersive mass flux can therefore be described, as in Burnett and Frind, 1987,

$$
\begin{aligned}
J_{dis} &= J_{mdis} + J_{dif} \tag{31} \\
&= -n\left(D_{mdis} + \tau D_m\right)\nabla C \tag{32} \\
&= -nD\nabla C \tag{33}
\end{aligned}
$$

where

$$
D = \begin{bmatrix}
D_{xx} & D_{xy} & D_{xz} \\
D_{yx} & D_{yy} & D_{yz} \\
D_{zx} & D_{zy} & D_{zz}
\end{bmatrix},
$$

$$
D_{ij} = \begin{cases}
\alpha_L \frac{v_x^2}{|v|} + \alpha_{TH} \frac{v_y^2}{|v|} + \alpha_{TV} \frac{v_z^2}{|v|} & i = j = x, \\
\alpha_L \frac{v_y^2}{|v|} + \alpha_{TH} \frac{v_x^2}{|v|} + \alpha_{TV} \frac{v_z^2}{|v|} + \tau D_m & i = j = y, \\
\alpha_L \frac{v_z^2}{|v|} + \alpha_{TV} \frac{v_y^2}{|v|} + \alpha_{TV} \frac{v_x^2}{|v|} + \tau D_m & i = j = z, \\
(\alpha_L - \alpha_{TH}) \frac{v_x v_y}{|v|} + \tau D_m & i = x, j = y, \\
(\alpha_L - \alpha_{TV}) \frac{v_x v_z}{|v|} & i = (x,z), j = (z,x), \\
(\alpha_L - \alpha_{TV}) \frac{v_y v_z}{|v|} & i = (y,z), j = (z,y),
\end{cases}
\tag{34}
$$

and

$$
|v| = \sqrt{v_x^2 + v_y^2 + v_x^2}.
\tag{35}
$$

For uniform flow, where $v = v_x$ and $v_y = v_z = 0$,

$$
\begin{aligned}
D_x &= D_L \\
&= \alpha_L v_x + \tau D_m \tag{36} \\
D_y &= D_{TH} \\
&= \alpha_{TH} v_x + \tau D_m \tag{37} \\
D_z &= D_{TV} \\
&= \alpha_{TV} v_x + \tau D_m. \tag{38}
\end{aligned}
$$

2.3 Advection

Solutes are transported by advection when they move along with the water in which they are dissolved. The expression for mass flux due to dispersion can be added to the expression for mass flux due to advection to give total mass flux due to both,

$$J = J_{mdis} + J_{dif} + J_{adv} \tag{39}$$

$$= J_{dis} + J_{adv} \tag{40}$$

$$= -nD\nabla C + nvC \tag{41}$$

$$= \left(-nD_{xx}\frac{\partial C}{\partial x} - nD_{xy}\frac{\partial C}{\partial y} - nD_{xz}\frac{\partial C}{\partial z} + nv_x C \right)\hat{i}$$

$$+ \left(-nD_{yx}\frac{\partial C}{\partial x} - nD_{yy}\frac{\partial C}{\partial y} - nD_{yz}\frac{\partial C}{\partial z} + nv_y C \right)\hat{j}$$

$$+ \left(-nD_{zx}\frac{\partial C}{\partial x} - nD_{zy}\frac{\partial C}{\partial y} - nD_{zz}\frac{\partial C}{\partial z} + nv_z C \right)\hat{k}. \tag{42}$$

For unidirectional flow

$$J = \left(-nD_{xx}\frac{\partial C}{\partial x} + nv_x C \right)\hat{i} + \left(-nD_{yy}\frac{\partial C}{\partial y} \right)\hat{j} + \left(-nD_{zz}\frac{\partial C}{\partial z} \right)\hat{k}. \tag{43}$$

3 Geochemistry

Geochemical phenomena significantly affect solute transport. As such, the geochemical attributes of various environments contribute differently to repository performance.

3.1 Saturated and Unsaturated Environments

Saturated repository concepts are found below the water table. Water permeates the rock.

Unsaturated repository concepts are found above or near the top of the water table. Water does not permeate the rock.

Current investigations are focused primarily on saturated environments.

3.2 Reducing and Oxidizing Environments[?]

Elements exist in various oxidation states, a positive or negative number refering to the charge of the atom due to the number of electrons it posesses. Oxidation refers to the increase of the oxidation state number of an element, and reduction is the opposite. That is, while oxidation is the chemical loss of electrons by an atom, reduction is the gaining of electrons by an atom.

The redox potential is the tendency in potential energy for an element to give up its electron and become more oxidized. This potential energy is measured relative to the potential for hydrogen atoms at unit concentration to lose electrons and become oxidized, in volts,

$$H_2 \rightarrow 2H^+ + 2e. \tag{44}$$

The potential for the redox equation in equation (44) is chosen to be 0 volts, such that for positive values of the redox potential, reactions tend to proceed in the oxidation direction. Accordingly, reactions proceed in the reduction direction for negative potentials.

Closed, saturated envrionments are reducing. Unsaturated environments and environments that are saturated and open are oxidizing.

The far field of most reducing environments are slightly oxidizing as they reach the zone near the overlying aquifer.

3.3 Salinity

Salinity affects sorption and solubility behaviors. It also expedites corrosion. Finally, salt is an important indicator of the historical flow at a site. Where should salinity information get incorporated in this model?

3.4 Sorption

Sorption is a factor that retards movement, in which solutes are incorporated into the surfaces of pores or fractures (adsorption) or incorporated into the rock matrix (absorption). More specificially, when water with some solute concentration, C_i, meets a porous medium or a granular solid, the reaction proceeds toward an equilibrium in which the solute mass has partitioned between the solution and the solid, such that,

$$S = \frac{V_w(C_i - C)}{m_s} \tag{45}$$

where

$$
\begin{aligned}
S &= \text{ mass sorbed on the surface } [kg/kg] \\
V_w &= \text{ volume of the solution } [m^3] \\
C_i &= \text{ initial concentration in the solution } [kg_m^3] \\
C &= \text{ equilibrium concentration in the solution } [kg/m^3] \\
m_s &= \text{ sediment mass } [kg].
\end{aligned}
$$

The function $S(C)$ is called a sorption isotherm. Two common forms for the sorption isotherm are

$$S = \begin{cases} \text{Freundlich :} & KC^n \\ \text{Langmuir :} & \frac{Q^0 KC}{1+KC} \end{cases} \tag{46}$$

where

$$
\begin{aligned}
K &= \text{ partition coefficient } [m^3/kg] \\
n &= \text{ shaping constant } [-]
\end{aligned}
$$

and

$$Q^0 = \text{ maximum sorptive capacity } [kg/kg].$$

If in the Freundlich isotherm,

$$n = 1, \tag{47}$$

then

$$S = K_d C \tag{48}$$

where

$$K_d = \text{ the distribution coefficient } [m^3/kg],$$

and the isotherm becomes very easy to incorporate into the mass transport equations, as in equation (62).

The simplest way to model sorption is with a linear isotherm and tabulated values. Sorption coefficients such as K_d are tabulated elementally because the character of the equilibrium reaction is element specific. For example, iodine has different sorption behavior than carbon. These coefficients are also host rock specific. That is, each element has different sorption behaviors in clay than in granite.

Geochemistry also plays a role, and sorption for some elements are higher in reducing environments. Sorption for some elements may be higher in oxidizing environments.

3.5   Solubility

The dissolution behavior of solutes in aqueous solutions is called its solubility. This behavior is limited by the solute's solubility limit, described by an equilibrium constant that depends upon temperature, water chemistry, and the properties of the element. The solubility constant for ordinary solutes, K_s gives units of concentration, $[kg/m^3]$, and can be determined algebraically by the law of mass action which gives the partitioning at equilibrium between reactants and products. For a reaction

$$cC + dD = yY + zZ, \tag{49}$$

where

$$
\begin{aligned}
c, d, y, z &= \text{ amount of respective constituent } [mol] \\
C, D &= \text{ reactants } [-] \\
Y, Z &= \text{ products } [-],
\end{aligned}
$$

the law of mass action gives

$$K = \frac{(Y)^y (Z)^z}{(C)^c (D)^d} \tag{50}$$

where

$$
\begin{aligned}
(X) &= \text{ the equilibrium molal concentration of X } [mol/m^3] \\
K &= \text{ the equilibrium constant } [-].
\end{aligned}
$$

The equillibrium constant for many reactions are known, and can be found in chemical tables. Thereafter, the solubility constraints of a solution at equilibrium can be found algebraically. In cases of salts that dissociate in aqueous solutions, this equilibrium constant is called the salt's solubility product K_{sp}.

This equillibrium model, however, is only appropriate for dilute situations, and nondilute solutions at partial equilibrium must be treated with an activity model by substituting the activities of the constituents for their molal concentrations,

$$[X] = \gamma_x (X) \tag{51}$$

where

$$
\begin{aligned}
[X] &= \text{ activity of X } [-] \\
\gamma_x &= \text{ activity coefficient of X} [-] \\
(X) &= \text{ molal concentration of X} [mol/m^3]
\end{aligned}
$$

such that

$$
\begin{aligned}
IAP &= \text{ Ion Activity Product } [-]. \\
&= \frac{[Y]^y [Z]^z}{[C]^c [D]^d} \tag{52}
\end{aligned}
$$

$$\tag{53}$$

The ration between the IAP and the equillibrium constant (IAP/K) quantifiesn the departure from equilibrium of a solution. This information is useful during the transient stage in which a solute is first introduced to a solution. When $IAP/K < 1$, the solution is undersaturated with respect to the products. When, conversely, $IAP/K > 1$, the solution is oversaturated and precipitation of solids in the volume will occur.

Two models of mass balance applicable to a control volume incorporating solubility limitation include the Ahn and Hedin models.

3.5.1 Ahn Solubility Limited Release Model

In the Ahn models, radionuclides with lower solubility coefficients are modeled with the solubility limited release model. Solubility values are assumed from TSPA for this model, and elements with a solubility of less than $5 \times 10^{-2} [mol/m^3]$ are taken to be 'low.' Elements in this 'low' category include Zr, Nb, Sn and some toxic actinides such as Th and Ra for an oxidizing, unsaturated environment similar to the Yucca Mountain Repository. It should be noted that in a reducing environment, the actinides are not as mobile, and the high and low solubility radionuclides will differ from this model. This model suggests that dissolution of radionuclides into the flowthrough water is dominated by diffusion, which is largely dependent upon the concentration gradient between the waste matrix and the water. The mass balance driving radionuclide release takes the form:

$$\dot{m}_i = 8 \epsilon D_e S_i L \sqrt{\frac{U r_0}{\pi D_e}} \tag{54}$$

where ϵ, U, r_0, and L are the geometric and hydrologic factors porosity, water velocity, waste package radius, and waste package length, respectively. D_e is the effective diffusion coefficient (m^2/yr) and S_i is the solubility (kg/m^3) of isotope i.

3.5.2 Hedin Solubility Limited Release Model

In the Hedin model of the waste matrix, the amount of solute available within the waste package is solved for, and for radionuclides with low solubility, the mass fraction released from the waste matrix is limited by a simplified description of their solubility. That is,

$$m_{1i}(t) \leq v_{1i}(t) C_{sol} \tag{55}$$

where the mass m_{1i} in $[kg]$ of a radionuclide i dissolved into the waste package void volume v_1 in $[m^3]$, at a time t, is limited by the solubility limit, the maximum concentration, C_{sol} in $[kg/m^3]$ at which that radionuclide is soluble [7].

Various things affect solubility. Temperature, salinity, etc.

A good model for solubility limitation is at the release boundary of the volume, for mixed volumes.

4 Solid Dissolution

Dissolution occurs after some kind of alteration and degradation.

Alteration is when some chemical reaction changes the characteristics of a material.

Give glass example.

Show that there are physical dissolution models being generated.

Waste form dissolution results may take place at a constant rate, a time dependent rate, or a physical model dependent on both static and dynamic parameters such as temperature, water velocity, or pH.

4.1 Waste Package Failure

Waste package failure is described best by a probability distribution such that a few packages can fail discretely at any one time.

It's also possible that a good model would fail all of the waste packages fractionally at some rate. This will affect both the water going in and the water coming out, but it's not clear to me how much this will affect those things.

5 Solute Transport in Porous Media

5.1 Derivation [3, 4]

Here we shall derive the general equation for solute transport in heterogeneous porous media.

As discussed in previous sections, mass transport by advection is driven by bulk water velocity, diffusion is the result of random thermal motion and tends to drive solutes down concentration gradients, and hydraulic dispersion results from heterogeneities in the water velocity field and drives accelerated mixing at the head of advection fronts.

Fundamentally, the effect of these phenomena on mass transport is captured by the conceptual mass conservation expression

$$\text{In} - \text{Out} = \text{Change in Storage} \tag{56}$$

which describes the mass balance within a reference volume of porous media.

By rearranging equation 56 and defining incoming and outflowing fluxes in a control volume, solute transport in a permeable medium of homogeneous porosity can be written (as in Schwartz and Zhang [1])

$$\frac{\partial nC}{\partial t} = -\nabla \cdot (F_c + F_{dc} + F_d) + m \tag{57}$$

where

$$
\begin{aligned}
n =\ & \text{solute accessible porosity } [\%] \\
C =\ & \text{concentration } [kg \cdot m^{-3}] \\
t =\ & \text{time } [s] \\
F_c =\ & \text{advective flow } [kg \cdot m^{-2} \cdot s^{-1}] \\
=\ & nvC \\
F_{dc} =\ & \text{dispersive flow } [kg \cdot m^{-2} \cdot s^{-1}] \\
=\ & \alpha nv \nabla C \\
F_d =\ & \text{diffusive flow } [kg \cdot m^{-2} \cdot s^{-1}] \\
=\ & nD_e \nabla C \\
m =\ & \text{solute source } [kg \cdot m^{-3} \cdot s^{-1}].
\end{aligned}
$$

In the expressions above,

$$
\begin{aligned}
v =\ & \text{advective velocity } [m \cdot s^{-1}] \\
\alpha =\ & \text{dispersivity } [m] \\
D_e =\ & \text{effective diffusion coefficient } [m^2 \cdot s^{-1}]
\end{aligned}
$$

and

$$n \cdot v =\ \text{Darcy flux } [m \cdot s^{-1}]. \tag{58}$$

The method by which the dominant solute transport mode (diffusive or advective) is determined for a particular porous medium is by use of the dimensionless Peclet number,

$$
\begin{aligned}
Pe &= \frac{nvL}{\alpha nv + D_e}, \\
&= \frac{\text{advective rate}}{\text{diffusive rate}}
\end{aligned}
\tag{59}
$$

where

$$L =\ \text{transport distance } [m].$$

For a high Pe number, advection is the dominant transport mode, while diffusive or dispersive transport dominates for a low Pe number. If one of these terms can be neglected, the solution is simplified.

Otherwise, the analytical expression in equation (57) will be the foundation of simplification by regression analyses for the radionuclide transport interface between components of the repository system model representing permeable porous media.

It is customary to define the combination of molecular diffusion and mechanical mixing as the dispersion tensor, D, such that the mass conservation equation becomes:

$$\nabla\left(nD\nabla C\right) - \nabla\left(nv\right) = \frac{\partial(nC)}{\partial t} \tag{60}$$

Adding sorption, by accounting for a change in mass storage,

$$\nabla\left(nD\nabla C\right) - \nabla\left(nv\right) = \frac{\partial(nC)}{\partial t} + \frac{\partial(s\rho_b)}{\partial t} \tag{61}$$

where

$$s = \text{sorbed phase concentration}$$
$$\rho_b = \text{bulk (dry) density } [kg/m^3].$$

If it is assumed that sorption can be approximated as a linear isotherm, reversible reaction,

$$\nabla\left(nD\nabla C\right) - \nabla\left(nv\right) = \frac{\partial(nC)}{\partial t} + \frac{\partial(s\rho_b)}{\partial t} \tag{62}$$

where

$$K_d = \text{species distribution coefficient.}$$
$$\tag{63}$$

This becomes

$$\nabla\left(nD\nabla C\right) - \nabla\left(nv\right) = \frac{\partial(nC)}{\partial t} + \frac{\partial(K_d C \rho_b)}{\partial t} \tag{64}$$

which, rearranged, gives

$$\nabla\left(nD\nabla C\right) - \nabla\left(nv\right) = \frac{\partial}{\partial t}\left(nC + K_d C \rho_b\right) \tag{65}$$

$$\nabla\left(nD\nabla C\right) - \nabla\left(nv\right) = \frac{\partial}{\partial t}\left(nC\left(1 + \frac{K_d \rho_b}{n}\right)\right). \tag{66}$$

In equations (66) it is clear that the storage term can be simplified with a retardation factor, such that if

$$R_f = \text{retardation factor} \tag{67}$$
$$= 1 + \frac{\rho_b K_d}{n} \tag{68}$$

then equation (??) can be written

$$\nabla\left(nD\nabla C\right) - \nabla\left(nv\right) = R_f \frac{\partial(nC)}{\partial t} \tag{69}$$

For uniform flow, the dispersion tensor, D, in equation 38 gives

$$D_x \frac{\partial^2 C}{\partial x^2} + D_y \frac{\partial^2 C}{\partial y^2} + D_z \frac{\partial^2 C}{\partial z^2} + v_x \frac{\partial C}{\partial x} = R_f \frac{\partial C}{\partial t}. \tag{70}$$

A special case of uniform flow, no flow, simplifies to the diffusion equation,

$$D_x \frac{\partial^2 C}{\partial x^2} + D_y \frac{\partial^2 C}{\partial y^2} + D_z \frac{\partial^2 C}{\partial z^2} = R_f \frac{\partial C}{\partial t}. \tag{71}$$

Solutions to these equations can be categorized by their boundary conditions. The first, or Dirichlet type boundary conditions define a specified species concentration on some section of the boundary of the representative volume,

$$C(x, y, z, t) = C_0(x, y, z, t) \text{ for } (x, y, z) \in \Gamma. \tag{72}$$

The second type or Neumann type boundary conditions describe a full set of concentration gradients at the boundary of the domain

$$\frac{\partial C(\vec{r}, t)}{\partial r} = nD\vec{J} \text{ for } \vec{r} \in \Gamma. \tag{73}$$

where

$$\vec{r} = \text{ position vector}$$
$$\Gamma = \text{ domain boundary}$$
$$\vec{J} = \text{ solute mass flux } [kg/m^2 \cdot s].$$

The third, Cauchy, defines a solute flux along a boundary,

$$vC(X, y, z, t) - D_x \frac{\partial C(x, y, z, t}{\partial x} = vg(x, y, z, t) \text{ for } (x, y, z) \in \Gamma \tag{74}$$

where

$$g(x, y, z, t) = \text{ arbirary flux profile} \tag{75}$$

this can also be written

$$-nD_{ij} \frac{\partial C}{\partial x_j} n_i + q_i n_i C = q_i n_i C_0. \tag{76}$$

5.2 Useful Known Solutions

Various solutions to the advection dispersion equation in Equation (70) have been published for both the first and third types of boundary conditions. The third, Cauchy type, is mass conservative, and will be the primary kind of boundary condition used at the source for this model.

5.2.1 One Dimensional Semi-Infinite Solution

The conceptual model in Figure 7 represents solute transport in one dimension with unidirectional flow and a semi-infinite boundary condition in the positive flow direction.

$$-D\frac{\partial C}{\partial x}\big|_{x=0} + vC = \begin{cases} vC_0 & t < t_0 \\ 0 & t > t_0 \end{cases} \qquad\qquad \frac{\partial C}{\partial x}\big|_{\infty} = 0$$

$$C(x,0) = C_i$$

$$x = 0 \qquad\qquad\qquad\qquad\qquad\qquad\qquad\qquad \infty$$

<div align="center">Figure 6: Case I, a one dimensional, semi-infinite model.</div>

With the boundary conditions

$$-D\frac{\partial C}{\partial x}\big|_{x=0} + v_x c = \begin{cases} vC_0 & (0 < t < t_0) \\ 0 & (t > t_0) \end{cases} \tag{77}$$

$$\frac{\partial C}{\partial x}\big|_{x=\infty} = 0 \tag{78}$$

and the initial condition

$$C(x,0) = C_i, \tag{79}$$

the solution is given as

$$C(x,t) = \begin{cases} C_i + (C_0 - C_i)\, A(x,t) & 0 < t < t_0 \\ C_i + (C_0 - C_i)\, A(x,t) - C_0 A(x, t - t_0) & t > t_0 \end{cases} \tag{80}$$

where

$$A(x,t) = \frac{1}{2}\,\mathrm{erfc}\left[\frac{Rx - vt}{2\sqrt{DRt}}\right] + \sqrt{\frac{v^2 t}{\pi DR}}\, e^{-\frac{(Rx - vt)^2}{4DRt}}. \tag{81}$$

5.2.2 One Dimensional Semi-Infinite Solution with Discrete Source

The conceptual model in Figure 7 represents solute transport in one dimension with unidirectional flow and a semi-infinite boundary condition in the positive flow direction.
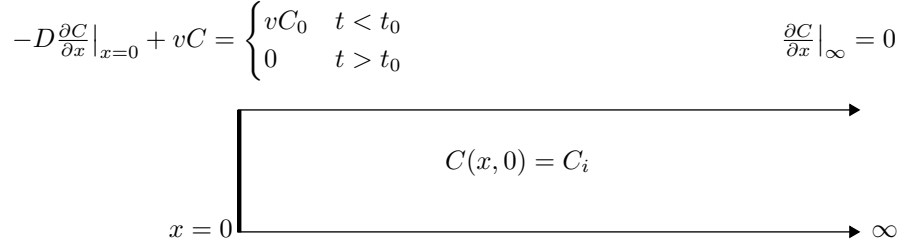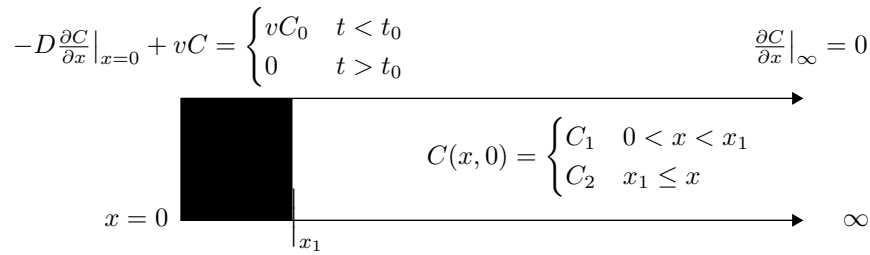
$$-D\frac{\partial C}{\partial x}\big|_{x=0} + vC = \begin{cases} vC_0 & t < t_0 \\ 0 & t > t_0 \end{cases} \qquad\qquad \frac{\partial C}{\partial x}\big|_{\infty} = 0$$

$$C(x,0) = \begin{cases} C_1 & 0 < x < x_1 \\ C_2 & x_1 \le x \end{cases}$$

$$x = 0 \qquad\qquad\qquad\qquad\qquad\qquad\qquad\qquad \infty$$
$$x_1$$

<div align="center">Figure 7: Case II, a one dimensional, semi-infinite model.</div>

With the boundary conditions

$$-D\frac{\partial C}{\partial x}\big|_{x=0} + v_x c = \begin{cases} vC_0 & (0 < t < t_0) \\ 0 & (t > t_0) \end{cases} \tag{82}$$

$$\frac{\partial C}{\partial x}\big|_{x=\infty} = 0 \tag{83}$$

and the initial condition

$$C(x, 0) = C_i, \tag{84}$$

the solution is given as

$$C(x, t) = \begin{cases} C_i + (C_0 - C_i) A(x, t) & 0 < t < t_0 \\ C_i + (C_0 - C_i) A(x, t) - C_0 A(x, t - t_0) & t > t_0 \end{cases} \tag{85}$$

where

$$A(x, t) = \frac{1}{2} \operatorname{erfc} \left[\frac{Rx - vt}{2\sqrt{DRt}} \right] + \sqrt{\frac{v^2 t}{\pi DR}} e^{-\frac{(Rx - vt)^2}{4DRt}}. \tag{86}$$

5.2.3 One Dimensional Finite Solution

The conceptual model in Figure 9 represents solute transport in one dimension with unidirectional flow and a finite boundary condition in the positive flow direction.
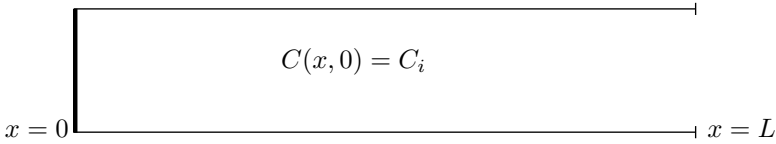
$$-D\frac{\partial C}{\partial x}\big|_{x=0} + vC = \begin{cases} vC_0 & t < t_0 \\ 0 & t > t_0 \end{cases} \qquad\qquad \frac{\partial C}{\partial x}\big|_{L} = 0$$

$$C(x, 0) = C_i$$

$$x = 0 \qquad\qquad\qquad\qquad\qquad\qquad\qquad\qquad x = L$$

Figure 8: Case III, a one dimensional, finite model.

With the boundary conditions

$$-D\frac{\partial C}{\partial x}\Big|_{x=0} + v_x c = \begin{cases} vC_0 & (0 < t < t_0) \\ 0 & (t > t_0) \end{cases} \tag{87}$$

$$\frac{\partial C}{\partial x}\Big|_{x=L} = 0 \tag{88}$$

and the initial condition

$$C(x, 0) = C_i, \tag{89}$$

the solution is given as

$$C(x, t) = \begin{cases} C_2 + (C_1 - C_2) A(x, t) + (C_0 - C_1) B(x, t) & 0 < t < t_0 \\ C_2 + (C_1 - C_2) A(x, t) + (C_0 - C_1) B(x, t) - C_0 B(x, t - t_0) & 0 < t < t_0 \end{cases} \tag{90}$$

where

$$A(x,t) = \frac{1}{2}\operatorname{erfc}\left[\frac{R(x-x_1)-vt}{2\sqrt{DRt}}\right] + \sqrt{\frac{v^2 t}{\pi DR}}e^{\left[\frac{vx}{D}-\frac{R}{4Dt}(x+x_1+\frac{vt}{R})^2\right]}$$

$$- \frac{1}{2}\left[1 + \frac{v(x+x_1)}{D} + \frac{v^2 t}{DR}\right]e^{\frac{vx}{D}}\operatorname{erfc}\left[\frac{R(x+x_1)+vt}{2\sqrt{DRt}}\right] \tag{91}$$

$$B(x,t) = \frac{1}{2}\operatorname{erfc}\left[\frac{Rx-vt}{2\sqrt{DRt}}\right] + \sqrt{\frac{v^2 t}{\pi DR}}e^{-\left[\frac{(Rx-vt)^2}{4DRt}\right]}$$

$$- \frac{1}{2}\left[1 + \frac{vx}{D} + \frac{v^2 t}{DR}\right]e^{\frac{vx}{D}}\operatorname{erfc}\left[\frac{Rx+vt}{2\sqrt{DRt}}\right]. \tag{92}$$

5.2.4 Three Dimensional Semi-Infinite Solution

The conceptual model in Figure 9 represents solute transport in three dimensions with unidirectional flow and a semi-infinite boundary condition in the positive flow direction. With the boundary conditions
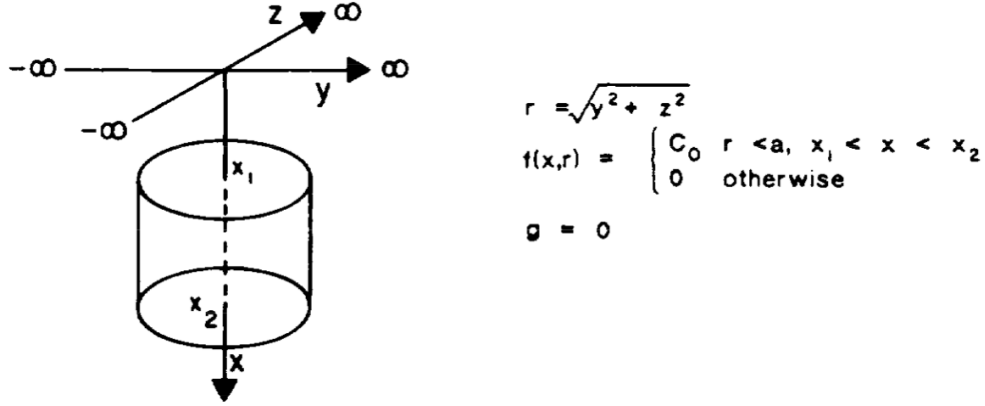

Figure 9: Case IV, a three dimensional, semi-infinite model.

$$-D\frac{\partial C}{\partial x}\Big|_{x=0} + v_x c = \begin{cases} vC_0 & (0 < t < t_0) \\ 0 & (t > t_0) \end{cases} \tag{93}$$

$$\frac{\partial C}{\partial x}\Big|_{x=L} = 0 \tag{94}$$

and the initial condition

$$C(x,0) = C_i, \tag{95}$$

the solution is given as

$$C(x,t) = C_0 \int_0^a \Lambda_6(t)\Xi(\rho,t)d\rho + \frac{\lambda}{2R}\int_0^t\int_0^\infty \Xi(\rho,\tau)\Lambda_4(\tau)d\rho d\tau \tag{96}$$

20

where

$$\Xi(\rho, \tau) = \frac{\rho R}{4 D_r \tau} e^{\left(-\frac{R(r^2 + \rho^2)}{4 D_r \tau}\right)} I_0\left(\frac{Rr\rho}{2 D_r \tau}\right), \tag{97}$$

$$I_0(x) = \sum_{m=0}^{\infty} \frac{1}{(m!)^2} \left(\frac{x}{2}\right)^{2m} \tag{98}$$

$$\Lambda_4(\tau) = \mathrm{erfc}\left[\frac{v\tau - Rx}{\sqrt{4 R D_x t}}\right] + \left(1 + \frac{v}{D_x}(x + v\tau/R)\right) e^{\left(\frac{vx}{D_x}\right)} \mathrm{erfc}\left[\frac{Rx + v\tau}{\sqrt{4 R D_x t}}\right]$$
$$- \sqrt{\frac{4 v^2 \tau}{\pi R D_x}} e^{-\left(\frac{(Rx - v\tau)^2}{\sqrt{4 R D_x \tau}}\right)}, \tag{99}$$

and

$$\Lambda_6(t) = e^{\frac{vx}{D_x}}\left[\left(1 + \frac{v}{D_x}(x + x_1 + vt/R)\right) \mathrm{erfc}\left[\frac{R(x + x_1) + vt}{\sqrt{4 R D_x t}}\right]\right.$$
$$- \left(1 + \frac{v}{D_x}(x_1 + x_2) + vt/R\right) \mathrm{erfc}\left[\frac{R(x + x_2) + vt}{\sqrt{4 R D_x t}}\right]\right]$$
$$+ \mathrm{erfc}\left[\frac{R(x - x_2) - vt}{\sqrt{4 R D_x t}}\right] i - \mathrm{erfc}\left[\frac{R(x - x_1) - vt}{\sqrt{4 R D_x t}}\right]$$
$$+ \sqrt{\frac{4 v^2 t}{\pi R D_x}} e^{\left(\frac{vx}{D_x}\right)}\left[e^{-\left(\frac{[R(x + x_2) + vt]^2}{4 R D_x t}\right)} - e^{-\left(\frac{[R(x + x_1) + vt]^2}{4 R D_x t}\right)}\right]. \tag{100}$$

Clearly, this functional form of the solution could be onerous to code. Thus, other solutions are being considered, including the lumped parameter model of radionuclide transport.

5.2.5 Lumped Parameter Model

For systems in which the flow can be assumed constant, it is possible to model a system of volumes as a connected lumped paramter models (Figure 10.
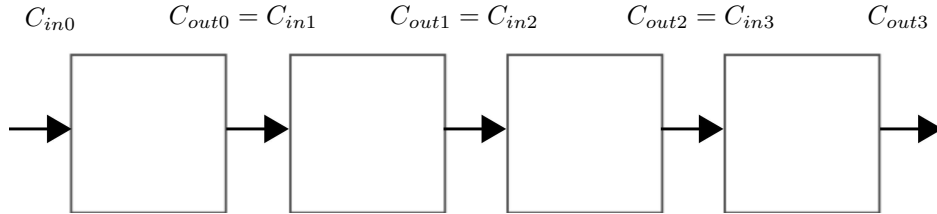
Figure 10: A system of volumes can be modeled as lumped parameter models in series.

The method by which each lumped parameter component is modeled is according to a relationship between the incoming concentration, $C_{in}(t)$, and the outgoing concentration, $C_{out}(t)$,

$$C_{out}(t) = \int_{-\infty}^{t} C_{in}(t') g(t - t') e^{-\lambda(t - t')} dt' \tag{101}$$

equivalently

$$C_{out}(t) = \int_{0}^{\infty} C_{in}(t - t') g(t') e^{-\lambda t'} dt' \tag{102}$$

where

$$
\begin{aligned}
t' &= \text{time of entry } [s] \\
t - t' &= \text{transit time } [s] \\
g(t - t') &= \text{response function, a.k.a. transit time distribution} [-]] \\
\lambda &= \text{radioactive decay constant, 1 to neglect} [s^{-1}]
\end{aligned}
\tag{103}
$$

Selection of the response function is usually based on experimental tracer results in the medium at hand. However, some functions used commonly in chemical engineering applications include the Piston Flow Model (PFM),

$$
g(t') = \delta(t' - t_t))
\tag{104}
$$

the Exponential Model (EM)

$$
g(t') = \frac{1}{t_t} e^{-\frac{t'}{t_t}}
\tag{105}
$$

and the Dispersion Model (DM),

$$
g(t') = \frac{\left[\left(\frac{t\pi t'}{t_t Pe}\right) \left(\frac{1}{t'}\right) e^{-\left(1 - \frac{t'}{t_t}\right)^2} \right]}{\frac{4t'}{t_t Pe}},
\tag{106}
$$

where

$$
\begin{aligned}
Pe &= \text{Peclet number } [-] \\
t_t &= \text{mean tracer age } [s] \\
&= t_w \text{ if there are no stagnant areas} \\
t_w &= \text{mean residence time of water} [s] \\
&= \frac{V_m}{Q} \\
&= \frac{x}{v_w} \\
&= \frac{x n_e}{v_f}
\end{aligned}
$$

in which

$$
\begin{aligned}
V_m &= \text{mobile water volume} [m^3] \\
Q &= t_w \text{ volumetric flow rate } [m^3/s \\
v_w &= \text{mean water velocity} [m/s] \\
v_f &= \text{Darcy Flux} [m/s]
\end{aligned}
$$

and

$$
n_e = \text{effective porosity} [\%].
$$

The latter of these, the Dispersion Model satisfies the one dimensional advection-dispersion equation, and is therefore the most physically relevant for this application.

The solutions to these for constant concentration at the source boundary give

$$
C(t) = \begin{cases}
PFM & C_0 e^{\lambda t_t} \\
EM & \frac{C_0}{1 + \lambda t_t} \\
DM & \frac{C_0 e^{\frac{Pe}{2}\sqrt{\left(1 - (1 + \frac{4\lambda t_t}{Pe})\right)}}}{2}
\end{cases}
\tag{107}
$$

5.3 Buffer Model

The buffer component is a long, but finite, cylindrical geometry with a series of cylindrical waste packages within it. These waste packages can be modeled as a single line source, a series of cylinders, or a series of points. If they are modeled as a single line source, the flux emitted by the line boundary will be expressed, in one dimension, as

$$vC_0 = v \sum_{p=1}^{p=P} C_p \tag{108}$$

where

$$
\begin{aligned}
vC_0 &= \text{ constant solute flux during the timestep } [kg/m^3/s < +check+ >] \\
C_p &= \text{ available concentration at waste package p } [kg/m^3] \\
P &= \text{ number of waste packages within the buffer cylinder } [\#].
\end{aligned}
$$

$$\tag{109}$$

If the line source is chosen, the one dimensional models in cases I, II, or III can be used, as can the lumped parameter model. In these cases, the flux at the inner buffer radius is described by the cylindrical source waste form. The concentration gradient can be defined as zero either at the outer buffer radius, or at infinity. These approximate solutions may not give significantly different results for many situations, but each will be investigated.

If alternatively, the waste packages are modeled as discrete cylinders, the buffer must also be modeled as a discrete cylinder within the broader, far field semi-infinite medium.

5.4 Far Field Solution

The three dimensional solution with a cylindrical source of constant flux is the most appropriate treatment for the boundary conditions of the far field component. With the length of the tunnels and outer radial dimension of the buffer, the far field can be modeled as a semi-infinite medium and the flux at the location of the perceived aquifer can be queried. In case IV, the flux escaping the cylindrical buffer will be an output of the buffer model. The concentration gradient is zero at infinity.

The far field may also be modeled as a lumped parameter system. It may either be modeled as a single lumped parameter component or as a series of smaller dimension lumped parameter components. For a homogeneous medium, the difference in accuracy between these two approaches will be zero, though for heterogeneous media for which local parameters are known, accuracy can be increased by decreased lumped parameter component length.

A corresponding one dimensional solution will be shown and its applicability will be justified.

The sides and bottoms of a two dimensional far field model are typically taken to be no flow boundaries. This garuntees that the only sources and sinks of water occur at the top surface, the aquifer.

5.5 Modeling Strategy

Comments on how to model this solution numerically will be discussed.

6 Thermal Transport

6.1 Decay Heat

The radioactive decay of isotopes in spent nuclear fuel produces heat.

Radioactivity is often expressed in Bequerels, or disintegrations per second,

$$1Bq = 1s^{-1}. \tag{110}$$

The activity of a radioactive sample is equal to the sum of the activities of each of its constituent isotopes,

$$A_{sample} = \sum_i^n A_i \tag{111}$$

$$= \sum_i^n \lambda_i N_i \tag{112}$$

where

$$
\begin{aligned}
A_{sample} &= \text{ disintegrations per second in the sample } [Bq] \\
A_i &= \text{ disintegrations per second due to isotope i } [Bq] \\
n &= \text{ the number of isotopes species in the sample } [-] \\
\lambda_i &= \text{ the decay constant of isotope i } [Bq] \\
N_i &= \text{ the number of atoms of isotope i in the sample } [-].
\end{aligned}
$$

The specific power, in $MeV \cdot s^{-1} \cdot g^{-1}$ generated by that sample at that second employs an isotope specific energy per disintegration factor,

$$P = \frac{E \lambda N_A}{M} [MeV \cdot s^{-1} \cdot g^{-1}] \tag{113}$$

where

$$
\begin{aligned}
E &= \text{ Energy release per disintegration } [Mev] \\
N_A &= \text{ Avogadro's number, } 6.022 \times 10^{-23} [mol^{-1}] \\
M &= \text{ Atomic weight } [amu].
\end{aligned}
$$

Energy in MeV can be converted to Watts by the conversion factor,

$$1[MeV \cdot s^{-1}] = 1.6 \times 10^{-13}[Watts], \tag{114}$$

such that

$$Q = 1.6 \times 10^{-13} \frac{E \lambda N_A}{M} [W(th)/g]. \tag{115}$$

6.2 Capacity Determination for Arbitrary Waste Form

Modeling heat will require a transient model capable of arriving at a heat based capacity quickly for an arbitrary waste stream.

6.3 Waste Stream Loading Density in Waste Forms

Either the user inputs the waste form loading density or the repository must determine how best to load the waste forms with waste .

6.4 Waste Package Loading Strategy in Repository

Either the user inputs the tunnel spacing and waste package spacing, or the repository must determine how best to space the tunnels and packages.

6.5 Solving for the Heat Evolution

This model should be capable of calculating the temperature field through the repository over time for a certain waste package layout.

6.6 Thermal Modeling Needs

The decay heat from nuclear material generates a significant heat source within a repository. In order to arrive at loading strategies that comply with thermal limits in the engineered barrier system and the geological medium, a thermal modeling capability must be included in the repository model. Such a model is also necessary to inform material and hydrologic phenomena that affect radionuclide transport and are thermally coupled.

Partitioning and transmutation of heat generating radionuclides within some fuel cycles will alter the heat evolution of the repository [?]. Thus, to distinguish between the repository heat evolution associated with various fuel cycles involving partitioning and transmutation, a repository analysis model, must at the very least, capture the decay heat behavior of dominant heat contributors. Plutonium, Americium, and their decay daughters dominate decay heat contribution within used nuclear fuels. Other contributing radionuclides include Cesium, Strontium, and Curium [?].

Thermal limits within a used nuclear fuel disposal system are waste form, package, and lithology dependent. The heat evolution of the repository constrains waste form loadings and package loadings as heat generated in the waste form is transported through the package. It also places requirements on the size, design, and loading strategy in a potential geological repository as that heat is deposited in the engineered barrier system and host lithology.

Thermal limits of various waste forms have their technical basis in the temperature dependence of isolation integrity of the waste form. Waste form alteration, degradation, and dissolution behavior is a function of heat in addtition to redox conditions and constrains loading density within the waste form.

Thermal limits of various engineered barrier systems similarly have a technical basis in the temperature dependent alteration, corrosion, degradation, and dissolution rates of the materials from whence they are constructed.

Thermal limits of the geologic environment can be based on the mechanical integrity of the rock as well as mineralogical, hydrologic and geochemical phenomena. The isolating characteristics of a geological environment are most sensitive to hydrologic and geochemical effects of thermal loading. Thus, heat load constraints are typically chosen to control hydrologic and geochemical response to thermal loading. In the United States, current regulations necessitate thermal limits in order to passively steward the repository's hydrologic and geochemical integrity against radionuclide release for the first 10,000 years of the repository.

The two heat load constraints that primarily determined the heat-based spent nuclear fuel (SNF) capacity limit in the Yucca Mountain Repository design, for example, are specific to unsaturated tuff. These are given here as an example of the type of regulatory constraints that this model will seek to capture for various lithologies.

The first Yucca Mountain heat load constraint is intended to promote constant drainage, thereby preventing episodic flow into waste package tunnels and subsequent contaminated water flow through the repository. It requires that the minimum temperature in the tuff between drifts be no more than the boiling temperature of water, which is $96°C$ at the altitude in question. For a repository with homogeneous waste composition in parallel drifts, this constraint limits the temperature exactly halfway between adjacent drifts, where the temperature is at a minimum.

The second constraint is intended to prevent high rock temperatures that could induce fractures and alteration of the rock. It stated that no part of the rock reach a temperature above $200°C$, and was effectively a limit on the temperature at the drift wall, where the rock temperature is a maximum.

Analogous constraints for a broader set of possible geological environments will depend on heat transport properties and geochemical behaviors of the rock matrix as well as its hydrologic state. Such constraints will affect the repository drift spacing, waste package spacing, and repository footprint among other parameters.

In addition to development of a concept of heat transport within the repository in order to meet heat load limitations, it is also necessary to model temperature gradients in the repository in order to support modeling of thermally dependent hydrologic and material phenomena. As mentioned above, waste form corrosion processes, waste form dissolution rates, diffusion coefficients, and the mechanical integrity of engineered

barriers and geologic environment are coupled with temperature behavior. Only a coarse time resolution will likely be necessary to capture that coupling however, since time evolution of repository heat is such that thermal coupling can typically be treated as quasi static for long time scales. [**?**].

6.7 Clay

Heat limits in clay are based on the domain of known behavior in clay and the tendency for bentonite fill material to lose its isolating properties with high temperatures [**?**, **?**]. Limits in clay are fairly low as the thermal conductivity of clay is typically lower than $2[W/m^\circ K]$[1].

The alteration of high smectite bentonite to non-expandable clays is a primary limitation for heat tolerance in the clay concept. The isolation characteristics of bentonite buffer materials are reduced after this alteration. The time integral of this phenomenon determines total bentonite alteration. While short bursts of heat might be allowable, because the bentonite will not alter immediately, the kinetic alteration into smectite clays is hastened by temperatures above approximately $100^\circ C$[**?**]. The Belgian program has considered increasing the thermal limit of the clay in the buffer region by adding graphite. Conversely, well understood behavior for argillaceous clay and bentonite buffer backfill is conservatively assumed by the Agence Nationale pour la gestion des Déchets RAdioactifs, the French National Agency for Radioactive Waste Management (ANDRA) assessment to occur only under $90^\circ C$, which is effectively a limit at the waste package interface with the bentonite buffer material[**?**] . The National Cooperative for the Disposal of Radioactive Waste (NAGRA) Opalinus Clay assessment less conservatively uses a maximum heat limit in the bentonite buffer of $125^\circ C$ [**?**] .

6.8 Granite

Granite repository concepts are limited by the bentonite buffer in a manner similar to that of clay. However, in the absence of the bentonite limitation, a thermal limit within the granite itself is greater than $200^\circ C$, limited by the increased risk of micro-cracking. This relatively high resistance to heat induced mechanical failure is due to the high thermal conductivity of granite, which is typically [2] found to be between 2.4 and 4 $[W/m \cdot^\circ K]$.

The effective thermal limit for granite disposal concepts, however, is usually related to the bentonite limit, which is conservatively assumed by the ANDRA assessment to occur under $90^\circ C$ at the waste package interface with the buffer material. Mechanical stresses and strains in the matrix due to heating at this level were analyzed by ANDRA and shown to have a negligible effect of flow behavior in granite. Similarly, thermo-hydraulic effects due to thermally induced fluid density changes are expected to be slight [**?**]. Similarly, for reasons of buffer isolation integrity, the Czech and Spanish granite disposal concepts both maintained a thermal limit at the waste package interface with the buffer of $100^\circ C$. [**?**]

Since the crystalline basement rock in which deep borehole concepts are envisioned is typically granite, the thermal behavior of the deep borehole environment is exactly similar to the granite case, except the bentonite buffer limitation is no longer applicable. Also, the $200^\circ C$ limitation in order to avoid microfissures could be shown to be irrelevant in light of the great distance to the surface. That is, even if the damage zone in the vicinity of the emplaced waste packages is enlarged significantly by high heat load, the kilometers of diffusion length to the surface will still dominate the isolation behavior of the repository.

6.9 Salt

Response of a salt repository to heat has a significant mechanical component. Bulk heating of a salt repository matrix causes coalescing of the salt surrounding the heat source. In the case of a nuclear waste repository, this phenomenon increases isolation capability of the salt. A heat limit, then, is difficult to characterize, but evolution of the heat in a salt environment is of great importance to radionuclide transport modeling.

---

[1] Belgium (ref. [**?**]) used values between 1.25 and 1.7 $[W/m \cdot^\circ K]$.
France (ref. [**?**]) used values between 1.9 and 2.7 $[W/m \cdot^\circ K]$.
Switzerland (ref. [**?**]) used 1.8 $[W/m \cdot^\circ K]$.
[2] Sweden (ref. [**?**]) used 3.4 - 4 $[W/m \cdot^\circ K]$ and 2.45 - 2.9 $[W/m \cdot^\circ K]$.
France (ref. [**?**]) used 2.4 - 3.8 $[W/m \cdot^\circ K]$.
Finland (ref. [**?**]) used 2.3 - 3.2 $[W/m \cdot^\circ K]$.

The German salt repository concept maintains a $180°C$ temperature limit. The technical basis for this limit has to do with the concern that at temperatures above $220°C$ the salt formation may release brines capable of facilitating radionuclide transport [**?**, **?**].

A model of temperature dependent salt coalescent behavior is in order. While coalescent phenomena has been observed within the Waste Isolation Pilot Plant (WIPP) facility, the emplaced material in WIPP is not high heat generating. Thus, high heat salt coalescent behavior warrants further study [**?**].

The Used Fuel Disposition (UFD) salt repository concept was based on some experience with construction and maintenance of the horizontal borings at WIPP. The current geometry involves emplacement of waste packages arranged at the corner of an alcove. This alcove is then backfilled with crushed salt. Notably, crushed salt has low conductivity, which increases the sensitivity of rock salt temperature on emplaced package temperature. However, as the crushed salt coalesces with heat over time, its thermal conductivity approaches that of intact salt. Further investigation toward a comprehensive model of the thermal behavior of dry salt has been recommended both domestically and internationally [**?**].

The behavior of moisture in a salt repository under high heat is also not well characterized . Though it is clear that the salt will creep and coalesce with increased temperature, the potential generation of brines within the salt at high heat is a pertinent issue for salt disposal characterization.

References

[1] F. W. Schwartz and H. Zhang, *Fundamentals of ground water*. 2003.

[2] H. Wang and M. P. Anderson, *Introduction to groundwater modeling*. Freeman, 1982.

[3] M. T. Van Genuchten, *Analytical solutions of the one-dimensional convective-dispersive solute transport equation*. No. 1661, US Dept. of Agriculture, Agricultural Research Service, 1982.

[4] F. J. Leij, T. H. Skaggs, and M. T. Van Genuchten, "Analytical solutions for solute transport in three-dimensional semi-infinite porous media," *Water resources research*, vol. 27, no. 10, p. 27192733, 1991.

[5] R. C. Heath, *Basic ground-water hydrology*, vol. 2220. US Geological Survey, 1983.

[6] JrPol, "Diffusion.svg." http://upload.wikimedia.org/wikipedia/commons/1/12/Diffusion.svg, Sept. 2011.

[7] A. Hedin, "Integrated analytic radionuclide transport model for a spent nuclear fuel repository in saturated fractured rock," *Nuclear Technology*, vol. 138, no. 2, 2002.